Modification of Na Channel Gating by an α Scorpion Toxin from *Tityus serrulatus*

G. E. KIRSCH, A. SKATTEBØL, L. D. POSSANI, and A. M. BROWN

From the Department of Physiology and Molecular Biophysics, Baylor College of Medicine, Houston, Texas 77030; and the Department of Biochemistry, Centre de Investigacion sobre Ingenieria Genetica y Biotechnologia, Universidad National Autonoma de Mexico, Mexico DF, 04510 Mexico

ABSTRACT The effects of TsIV-5, a toxin isolated from the Brazilian scorpion *Tityus serrulatus*, on whole-cell and single-channel Na currents were determined in N18 neuroblastoma cells. In whole-cell records at a test potential of −10 mV, external application of 500 nM TsIV-5 slowed inactivation 20-fold and increased peak current by about one-third without changing time-to-peak. Both the steady-state activation and inactivation curves were shifted to more negative potentials. Other α scorpion toxins produce similar effects but the single-channel mechanism is not known. TsIV-5 caused a voltage-dependent prolongation of mean single-channel open time such that at a test potential of −60 mV no change was observed, whereas at −20 mV mean open time increased about threefold and prolonged bursting was observed. Macroscopic current reconstructed from summed single-channel records showed a characteristic toxin-induced potentiation of peak current and a 20-fold slowing of the decay phase. TsIV-5 does not discriminate between tissue-specific Na channel subtypes. Prolonged open times and bursting were also observed in toxin-treated Na channels from rat ventricular myocytes, rat cortical neurons, and mouse skeletal muscle. The toxin effects are shown to be consistent with a kinetic model in which TsIV-5 selectively interferes with the ability of the channel to reach the inactivated state.

INTRODUCTION

Na channels, which generate the nerve impulse, are the sites of action of small polypeptide neurotoxins isolated from scorpion venom. These toxins have proven useful as probes of Na channel structure and function (recently reviewed by Strichartz et al., 1987). The venom of the Brazilian scorpion *Tityus serrulatus* contains several Na channel toxins including Ts-γ and TsIV-5, which can be distinguished on the basis of their NH_2-terminal amino acid sequences (Possani et al., 1985). TsIV-5 may be identical to Tityustoxin, which was isolated, but not sequenced, by Gomez and Diniz (1966), and was later shown to potentiate Na influx in rat brain synaptosomes (Bar-

Address reprint requests to Dr. G. E. Kirsch, Department of Physiology and Molecular Biophysics, Baylor College of Medicine, One Baylor Plaza, Houston, TX 77030.

J. GEN. PHYSIOL. © The Rockefeller University Press · 0022-1295/89/01/0067/17 $2.00
Volume 93 January 1989 67–83

hanin et al., 1982) and rat heart (Renaud et al., 1986). The electrophysiological effects of Ts-γ on Na channels have been characterized by previous work from our laboratory (Yatani et al., 1988) and others (Vijverberg et al., 1984). In the present paper we describe the mechanism of action of TsIV-5 which is markedly different from that of Ts-γ.

Scorpion toxins have been divided into α and β classes depending on their mode of action and ability to participate in competitive binding interactions (Couraud et al., 1982; Wheeler et al., 1983). α toxins have been isolated from the venom of North African and Middle Eastern scorpions, whereas β toxins come from the venom of North and South American scorpions. Both toxins modify Na channel gating; α toxins interfere with the ability of channels to inactivate upon prolonged depolarization, whereas β toxins shift the threshold for channel activation to more negative potentials and interfere with channel closing upon repolarization. The identification of toxin effects with specific modifications of Na channel gating is based on measurement of macroscopic Na conductance, the interpretation of which has undergone recent revision based in part on the study of currents recorded from single Na channels (Aldrich et al., 1983; Vandenberg and Horn, 1984). In particular, the inactivation phase of macroscopic Na current has been shown at the single-channel level to contain an important contribution from delayed activation of channels (Aldrich et al., 1983). Thus, the distinction between activation and inactivation has become blurred at the single-channel level, hence the identification of toxin sites of action with either the activation or inactivation gates needs to be reexamined. In the present study we report the effects of TsIV-5 on both macroscopic and single-channel Na currents in mammalian cells. TsIV-5 drastically slows the inactivation, in a manner similar to that of α toxins. At the single-channel level TsIV-5 prolongs the dwell time of channels in the open state by preventing open channels from closing and by facilitating the reopening of closed channels. These effects are shown to be consistent with a kinetic model in which TsIV-5 interferes with the ability of the channel to reach the inactivated state.

METHODS

Solutions and Drugs

TsIV-5 was purified as described previously (Possani et al., 1981). Briefly, venom solution was fractionated by gel filtration on Sephadex G-50 followed by ion exchange chromatography in two stages. First, fraction IV from the Sephadex column was applied to a carboxymethylcellulose column equilibrated with 20 mM ammonium acetate buffer at pH 4.7, and eluted with a salt gradient from 0 to 0.55 M NaCl. In the second step, fraction IV-5 was dialyzed and rechromatographed in a column equilibrated with 50 mM sodium phosphate buffer at pH 6.0, the major component of which was toxin TsIV-5. Homogeneity of the toxin was verified by polyacrylamide gel electrophoresis and NH_2-terminal amino acid sequencing. A stock solution of toxin in distilled water was stored at −20°C and diluted 25–100-fold in experimental solutions. External solution (bath) for whole-cell recording contained (in millimolar): 34 NaCl, 210 *N*-methyl-D-glucamine (NMDG), 5.4 KCl, 1.3 $CaCl_2$, 1.0 $MgCl_2$, 5 glucose, 5 HEPES, pH 7.4. Internal (pipette) solution for whole-cell recording contained (in millimolar): 110 NMDG, 160 HEPES, 10 CsF, 20 EGTA, pH 7.4. External solution (bath) for single-channel recording contained (in millimolar): 137 sodium methanesulfonate, 5.4 KCl, 1.0

$MgCl_2$, 2.0 $CaCl_2$, 10 glucose, 10 HEPES, pH 7.4. Internal (pipette) solution for single-channel recording contained (in millimolar): 120 CsF, 11 EGTA, 2 $McCl_2$, 10 HEPES, pH 7.4.

Cell Culture

Neuroblastoma N18 cells were plated on poly-D-lysine–coated glass cover slips in a medium consisting of 5% fetal calf serum and 95% Dulbecco's modified Eagle's medium (DMEM-5 FCS), and grown to a density of 2×10^4 cells/ml. Serum-containing medium was removed and replaced with DMEM supplemented with 1 mM dibutyryl cyclic AMP. After 2 d, isolated round cells (diameter, ~20 μm), were selected for electrophysiological recording.

Primary heart cell cultures were prepared from neonatal rats (1–3 d old) as described previously (Yatani et al., 1988). Briefly, ventricular pieces were incubated at 37°C for 5 min in Ca-free Hank's solution containing 0.5% typsin (T-0134; Sigma Chemical Co., St. Louis, MO). Supernatant was removed and the pelleted cells were added to DMEM-10 FCS. Resuspended cells were seeded on glass coverslips and incubated at 37°C in 5% CO_2-95% O_2 atmosphere. Recording was performed 1–2 d after seeding.

Neuronal cell cultures were prepared from neonatal rat brain cortex and dissociated into single cells by passing tissue suspensions through 0.04-mm nylon mesh filter. Cells were pelleted from the filtrate, resuspended, and plated on glass coverslips. After a 24-h incubation at 37°C in DMEM-10 FCS, the cells were placed in a serum-free defined medium, selective for neuronal growth (DMEM supplemented with insulin, transferrin, progesterone, putrescine, and sodium selenite). Recording was performed 7–14 d after seeding.

Mouse skeletal muscle-derived (C2) cells were seeded on poly-D-lysine–coated coverslips in a growth medium consisting of Ham's F12 nutrient medium supplemented with 20% FCS, and grown to a density of 2.5×10^4 cells/ml. After 2 d, FCS-containing medium was replaced with DMEM supplemented with 2% horse serum to induce differentiation. After 7 d in culture, striated myotubes were selected for electrophysiological recording.

Electrophysiological Recording

Patch-clamp recording was performed using techniques described previously (Hamill et al., 1981; Lux and Brown, 1984). Whole-cell Na currents were recorded using micropipettes (Corning /052 glass; Corning Glass Works, Corning, NY) fire-polished to a resistance 0.6–1.0 MΩ when filled with internal solution. Membrane currents evoked by 15-ms test pulses from a holding potential of −80 mV were measured using an EPC-7 (List Co., Darmstadt, FRG) amplifier. The records were filtered at 3.15 kHz (−3 dB), digitized with 12-bit resolution at 25 kHz, and stored on magnetic disk under computer control (LSI 11/23; Digital Equipment Co., Marlboro, MA). Test pulses were preceded by 100-ms hyperpolarizing prepulses to remove resting inactivation. Linear capacitative and leakage currents were corrected off-line by the subtraction of scaled currents evoked by hyperpolarizing pulses. The effect of series resistance was partially compensated electronically (Hodgkin and Huxley, 1952). External Na was decreased to 34 mM to improve voltage control and to diminish the effect of residual uncompensated series resistance. Whole-cell recording was performed at room temperature, 22–23°C.

Single-channel Na currents were recorded from outside-out membrane patches using Sylgard-coated micropipettes (Corning 7052 glass) fire-polished to resistance of 8–15 MΩ. External solution consisted of low-chloride Tyrodes solution that provided lower baseline noise than normal Tyrodes. The pipette-filling solution consisted primarily of CsF, which increased Na channel longevity in excised patches. Experiments were performed at 10°C to improve the resolution of the measurement of channel kinetics.

Single-channel records evoked by 140-ms depolarizing pulses were obtained using an Axo-

patch (Axon Instruments, Inc., Burlingame, CA) amplifier and stored on videocassette tape at a bandwidth of 16 kHz. The data were digitized off-line under computer control with 12-bit resolution at a sample rate 10 kHz after low-pass filtering at 3.15 kHz (−3 dB) using a four-pole Bessel filter (Ithaco, Inc., Ithaca, NY). Digitized records were corrected off-line for linear leakage and capacitative currents by subtracting the average of null traces that contained no openings, then digitally filtering them using a zero-phase four-pole low-pass Bessel filter at 1.4 kHz before level detection. Transitions between closed and open levels were determined using a threshold detection program in which opening threshold was set at half-maximum amplitude of single-unit opening. Computer-detected openings were confirmed by visual observation and used to generate idealized records from which histograms of amplitude, waiting, closed, and open time distributions were constructed. Amplitude histograms were fit by Gaussian functions using a χ^2 nonlinear regression routine. Single units of <0.4-ms duration were excluded from amplitude histograms to avoid the truncation error introduced by the limited frequency response of the recording system. Waiting time distributions were obtained by determining the latency between the beginning of each test pulse and the first channel event detected in the record. The distributions were corrected for the number of channels in the patch (estimated from channel overlap at potentials −20 to −10 mV) by the method of Patlak and Horn (1982). Open-time histograms were constructed from data sets in which events consisting of overlapping multiple single units were systematically excluded. Prepulse potentials were adjusted to ensure that the fraction of such events was <15% of the total at a given test potential to minimize the bias introduced by excluding overlaps. Openings of <0.4-ms duration were excluded from curve fitting to avoid errors arising from recording limitations. The sum of idealized records at a given test potential were used to reconstruct macroscopic currents and to determine the probability of opening. Mean open times, closed times, waiting times, and macroscopic current decay time constants were calculated by fitting the data to the sum of exponential decay functions using a maximum likelihood estimate. The accuracy of fitting biexponential models in preference to monoexponential ones was evaluated by a ratio of variance test (F test, $P = 0.05$). Where appropriate, data are expressed as mean ± SE. Significance of differences between means was evaluated using a two-tailed Student's t test ($P = 0.05$).

RESULTS

Whole-Cell Currents

External application of 5×10^{-7} M TsIV-5 to N18 cells in the whole-cell voltage-clamp mode resulted in a marked prolongation of the decay phase of macroscopic Na current and a modest increase in peak current as shown in Fig. 1. The superimposed smooth curves show exponential fits to the decay of Na current. The control curve was fit by a single exponential with a time constant of 0.43 ms, whereas two time constants, 1.6 and 12.2 ms, were required after toxin treatment. No change in the rising phase of the current is apparent at this potential. The onset of the effect required 10–20 min to reach steady state. In the traditional view of Na channel gating, the toxin appears to interfere selectively with inactivation without affecting activation. Assuming an overlap between the time course of activation and inactivation, the increase in peak current can be explained by the delayed onset of inactivation. In other experiments (not shown) the toxin was found to be specific for the Na channel; no effects were seen under ionic conditions that isolate the potassium-selective components of the total membrane conductance.

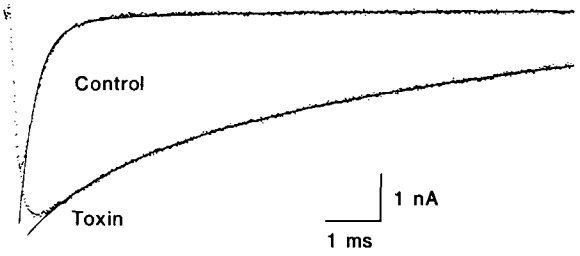

FIGURE 1. Whole-cell Na currents before and 20 min after application of 5×10^{-7} M TsIV-5. Test pulse potential, −10 mV; prepulse potential, −100 mV; and holding potential, −80 mV. Digitized data superimposed on smooth curves fit with exponential decay functions with the following parameters. Control time constant, 0.43 ms; toxin time constants (and weighting factors), 1.6 ms (0.3) and 12.2 ms (0.7). Temperature was 22.3°C.

Potentiation of peak Na conductance was variable but in no case were the toxin-modified currents smaller than in control. This variability may arise from a tendency of toxin-bound channels to pass into an inactive state at the holding potential. Withdrawal of these channels from the activatable pool partially offsets the toxin-induced potentiation of peak current. An experiment that illustrates this effect is shown in Fig. 2. Cells were maintained for 3 min at various holding potentials and the amount of activatable current was assessed from the peak currents evoked by test pulses to −10 mV. Each test pulse was preceded by a 100-ms prepulse to −120 mV to reset fast components of inactivation. In the absence of toxin no change in peak currents was observed in this range of holding potentials, but in the presence of toxin (Fig. 2) a shift in holding potential from −120 to −80 mV resulted in a 50% decrease in peak current. The waveform of the test pulse currents, however, was virtually identical regardless of the holding potential, indicating that toxin binding to the channel is insensitive to holding potential in this range.

The effects of toxin on the peak current-voltage relationship is shown in Fig. 3, the main features being the marked toxin-induced increase in peak conductance in the test potential range −50 to 20 mV (Fig. 3 *C*), and the large increase in residual current that failed to inactivate by the end of the test pulse.

TsIV-5 altered the voltage-dependence of both the steady-state and kinetic properties of Na inactivation as shown in Fig. 4. Steady-state inactivation was determined by a conventional two-pulse protocol in which a 100-ms prepulse to various conditioning potentials was immediately followed by a brief test pulse to a fixed potential. The prepulse allowed inactivation to reach a steady state and the test pulse served to

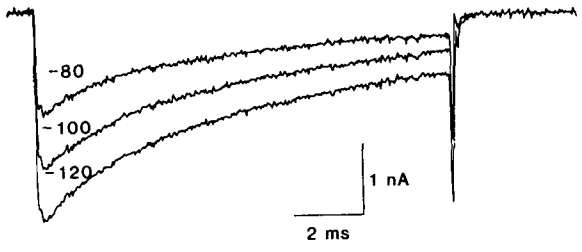

FIGURE 2. Effect of holding potential on toxin-modified Na current. Cell was held at −80 mV and equilibrated in TsIV-5 (5×10^{-7} M) for 20 min. Holding potential was reset to each of the levels indicated for a period of 3 min. Na currents were evoked by test pulses to −10 mV (prepulse, −120 mV, 100 ms).

assess the fraction of current that failed to inactivate during the prepulse. The ratio of peak test pulse current to maximum current, plotted as a function of prepulse potential (Fig 4 *A*), yields the steady-state voltage dependence of fast inactivation (Hodgkin and Huxley, 1952). TsIV-5 shifted the inactivation curve ~−3 mV and altered its shape such that a foot was observed at potentials more positive than −50 mV. The foot arises from prepulse Na currents that do not inactivate during the 100-ms pulse duration. At prepulse potentials below activation threshold, however,

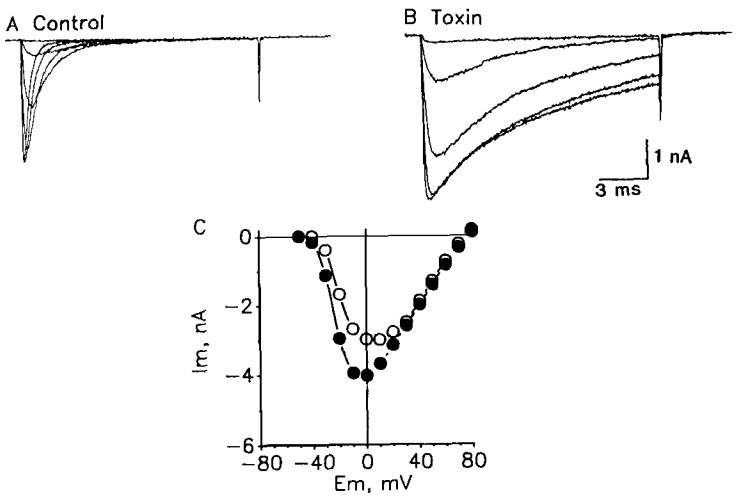

FIGURE 3. Current-voltage relationship before and after equilibration of 5×10^{-7} M TsIV-5. Test potentials ranged from −60 to +80 mV in 10-mV increments; for clarity only the records −60 to −10 are shown in *A* and *B*. Holding potential was −80 mV. In *C*, peak currents before (open circles) and after (filled circles) toxin treatment, are plotted as a function of test potential.

toxin-modified channels show significant inactivation, which suggests that the pathway from resting to inactivated states remains available even in the toxin-modified channels. Thus, a plausible explanation of TsIV-5 action is that the toxin interferes mainly with the transition from open-to-inactivated states without affecting the closed-to-open transition. Considerable insight into the nature of the toxin-induced modification of channel gating can be gained from examining single-channel currents as shown in the next section.

Single-Channel Currents

Single-channel records were obtained from eight membrane patches under control conditions and five patches treated with 2×10^{-6} M TsIV-5. Patches were allowed to equilibrate with toxin for at least 10 min before starting data collection. To conserve our supply of toxin only two patches were examined both before and after toxin application, and the results from one of the latter were analyzed in detail. Three other patches were obtained from cells that had already equilibrated with toxin; these results appear in the pooled data (e.g., Fig. 7 *A*) and in Fig. 9. Unlike

the whole-cell records that were obtained at room temperature, the single-channel data were taken at 9–11°C to improve the resolution of gating kinetics.

Fig. 5 shows typical single-channel records obtained under normal (Fig. 5, *A* and *C*) conditions and in the presence of TsIV-5 (Fig. 5, *B* and *D*). In control records single-channel openings are clustered at the beginning of the test step corresponding to the transient nature of membrane Na conductance. In this patch four channels were present based on the maximum observed number of overlapping unitary events. At −50 mV (Fig. 5 *C*), channels generally opened only once and these events had longer first latencies (delay between the onset of the test step, arrow in Fig. 5,

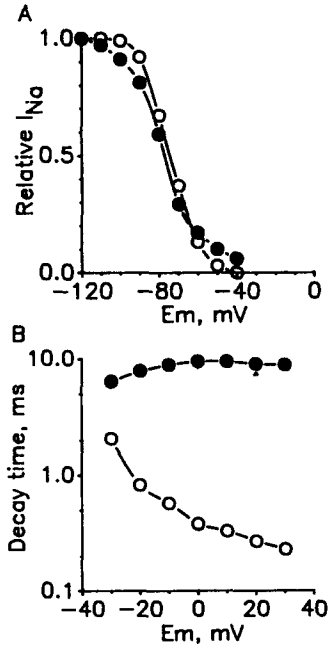

FIGURE 4. Voltage dependence of inactivation before (open circles) and after (filled circles) TsIV-5 treatment (5×10^{-7} M). Steady-state inactivation (*A*) was measured using a two-pulse protocol in which a 100-ms prepulse to various conditioning potentials immediately preceded a 15-ms test pulse to 0 mV. The prepulse allowed inactivation to reach a steady state and the test pulse served to assess the fraction of current that failed to inactivate during the prepulse. The ratio of peak test pulse current to maximum current (prepulse, −120 mV) is plotted as a function of prepulse potential. The time course of Na current decay (*B*) is plotted semilogarithmically as a function of test potential. Data from three cells are pooled and error bars omitted where smaller than symbols. Decay time is the weighted average of the time constants obtained by fitting a biexponential function to the decay phase of the currents. Fitting was performed by a nonlinear least-squares algorithm.

and the first opening in each trace), compared with openings evoked by test steps to −20 mV (Fig. 5 *A*). This results in a slower time course of activation at −50 mV, compared with −20 mV. However, at both potentials channels passed into the inactivated state within 20 ms of pulse onset. Not shown are null traces in which channels presumably passed directly from closed to inactivated states. Strikingly different kinetic features were observed after toxin application. Modified channels opened repetitively and the dwell time of each opening was longer on average than normal. Furthermore, at test potentials near activation threshold (Fig. 5 *D*), longer than normal first latencies were occasionally observed. The toxin did not alter single-channel conductance (9.2 ± 0.13 and 9.6 ± 0.40 pS, respectively, in control and toxin).

The effects of TsIV-5 on channel dwell time in the open state were quantified by constructing open-time histograms as shown in Fig. 6. Before toxin application the open-time histogram was accurately described by a monoexponential decay with time constants of 1.1 and 1.8 ms, respectively, at test potentials of −20 and −50 mV. At −20 mV in the presence of toxin (Fig. 6 *B*) the open-time histogram was more accurately described by the sum of two exponential functions (τ_1 = 1.0 ms, τ_2 = 6.6 ms), which suggests that either the channel population contains both modified and unmodified channels or that the toxin-modified channels have two open states. Since unmodified channels inactivate within 20 ms, we constructed histograms of openings that occurred after 20 ms. Such histograms (not shown) also

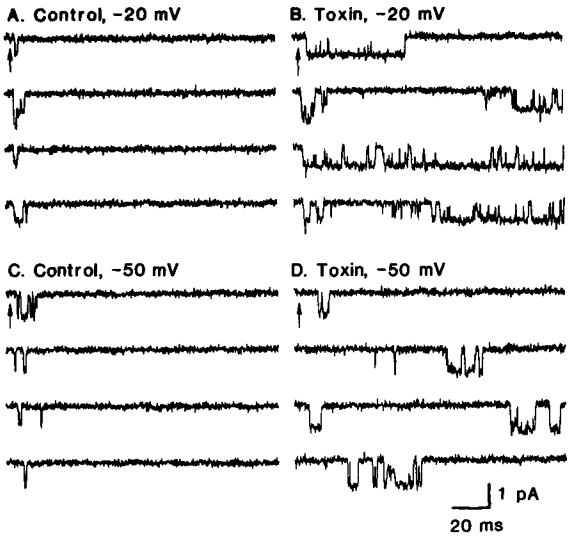

FIGURE 5. Single Na channel currents in an outside-out patch from membrane of N18 cell in the presence (*B* and *D*) and absence (*A* and *C*) of TsIV-5 (2×10^{-6} M). Each panel shows records evoked by 140-ms test pulses (onset marked by arrow) to −20 (*A* and *B*) and −50 (*C* and *D*) mV, from a holding potential of −90 mV. Each test pulse was preceded by a 100-ms prepulse to −120 mV to remove resting inactivation. End of trace coincides with end of test pulse. Pulses were delivered at 0.6 Hz. Channel openings are indicated by downward deflections. Records were filtered at 3.15 kHz (−3 dB), digitized at 100 kHz and digitally filtered at 1.4 kHz. Capacitance and leakage currents were minimized by using Sylgard-coated electrodes and electronic compensation. Final correction was made by digital subtraction of traces containing no activity. Null traces represented 25, 12, 46, and 43% of the total recorded in the patch represented, respectively, by *A*, *B*, *C*, and *D*. Temperature was 10.4°C.

required a biexponential distribution to accurately fit the data (time constants 1.9 and 10.5 ms) which suggests that the toxin-modified channels have both long (accounting for 37% of the area of the open-time histogram) and short-lived open states (63%).

At a test potential of − 50 mV (Fig 6, *C* and *D*) the open-time histograms obtained before and after toxin application were nearly indistinguishable. Both could be accurately fit by monophasic decays with time constants of 1.8 and 2.3 ms, respectively, in control and toxin. Thus, the toxin-induced prolongation of mean open time appears to depend on test potential. Clearly, at −50 mV the gating mechanism that closes the channel is less susceptible to toxin modification than at −20 mV. As shown later, this may be due to selective modification of the open-to-inactivated transition.

Pooled open-time data from all patches over a range of test potentials (Fig. 7) were obtained by calculating the arithmetic mean at each potential and combining the averages from different patches. In control patches mean open time was <2 ms independent of test potential, whereas in toxin-treated patches mean open time increased from control levels at −60 mV to roughly three times control at −20 mV. As shown in Fig 7 *B*, this increase in open time by itself does not entirely explain the prolonged decay of macroscopic currents. In the reconstructed macroscopic currents, obtained by summing several hundred single-channel records (same patch as in Fig. 5), current through toxin-modified channels decayed roughly 20 times more slowly than control. An explanation of this effect is the prolonged bursting that is a prominent feature of toxin-modified channels.

We measured burst durations in records such as those in Fig. 5 *B*, from which traces containing overlapping openings of multiple channels were systematically

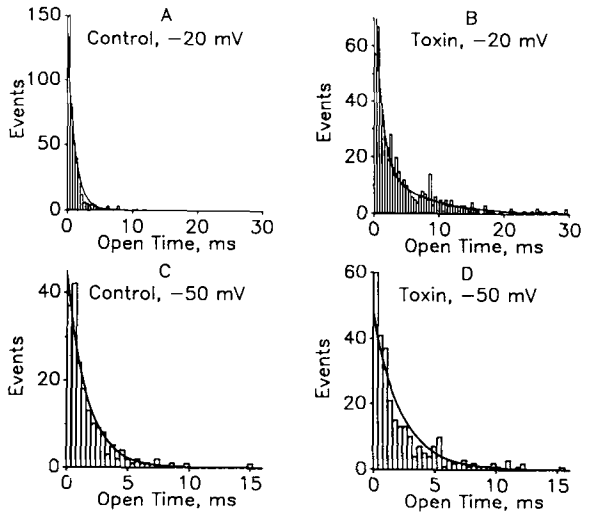

FIGURE 6. Open-time histograms in absence (*A–C*) and presence of (*B–D*) of TsIV-5. Same experiment as in Fig. 5. Simultaneous openings of more than one channel were excluded. Histograms were fit to exponential distributions using a Marquardt algorithm and a maximum likelihood estimator. In *A*, *C*, and *D*, monoexponential distributions (τ = 1.12, 2.24, and 1.78 ms, respectively) accurately fit the data. In *B*, a biexponential distribution was required, with time constants (and weighting factors): 1.0 ms (0.4) and 6.6 ms (0.6).

excluded. The frequency distributions of closed times in normal and toxin-modified channels were evaluated at a test potential of −20 mV, and each of the resulting histograms was found to contain two major components consisting of closings with mean durations of 0.8 and 25.0 ms, and 0.9 and 56.6 ms, respectively, in toxin and control. We estimated the minimum closed time within a burst to be 3 ms (Colquhoun and Sakmann, 1985). Bursts defined in this way were assumed to arise from the repetitive opening and closing of a single channel. Mean burst duration in toxin-modified channels was 30 ms (average number of openings per burst was 4.0) compared with 2.4 ms (average number of openings per burst was 1.3) in control. The 20-fold increase in the duration of the decay phase of toxin-modified macroscopic current, therefore, is due to the combined effects of increased mean open time and burst duration.

The reconstructed macroscopic traces in Fig. 7 *B* also show that the rising phase of Na current in both the control and toxin-treated patch were superimposable at a

test potential of −20 mV. We examined the voltage dependence of this effect in more detail by constructing cumulative frequency distributions of latency-to-first-opening (waiting) time (Fig. 8). The shape of such plots should correspond to the time course of channel activation. Thus, under normal conditions the initial rising phase of the waiting-time histogram became steeper as the test potential increased from −50 (Fig. 8 *B*) to −20 mV (Fig. 8 *A*), which corresponds to the voltage-

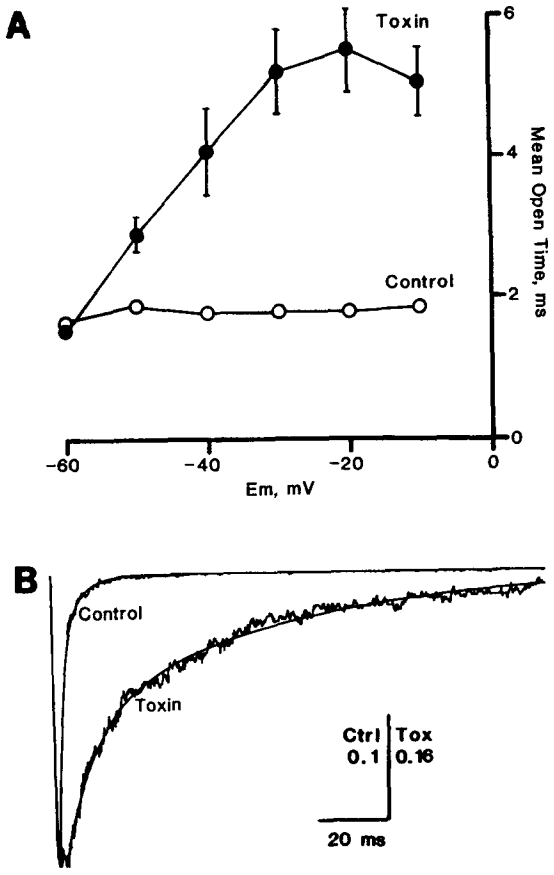

FIGURE 7. Voltage dependence of mean open times (*A*) and kinetic features of reconstructed macroscopic currents (*B*). Mean open times were calculated as in Fig. 6. A weighted average of time constants was calculated from biexponential open-time distributions. (*A*) Pooled mean open times under control (open circles) and in the presence of TsIV-5 (filled circles, 2×10^{-6} M) are plotted as a function of test potentials. Error bars omitted where smaller than symbols. (*B*) Summed single-channel records (same experiment as in Fig. 5) in presence and absence of TsIV-5 at a test potential of −20 mV are scaled to the same peak to illustrate toxin-induced changes in macroscopic currents. Vertical calibration in *B* gives scale factor in terms of probability of single-channel opening. Decay phase of both records was accurately described by biexponential functions. Control time constants (and weighting factors), 1.35 ms (0.85) and 4.8 ms (0.15); toxin time constants, 8.23 ms (0.45) and 57.5 ms (0.55). Temperature was 10.4°C.

dependent increase in activation rate. At a test potential of − 20 mV (Fig. 8) TsIV-5 had less effect on the shape of the waiting-time histogram. In both toxin and normal conditions the histograms could be fit by a function consisting of the sum of two exponentials (τ_1 = 0.7 and 0.6, τ_2 = 6.1 and 9.2, respectively, in toxin and control). The differences in the plateau reflects the ~60% increase in probability of opening (Fig. 7 *B*) of the toxin-modified channel. At a test potential of −50 mV the cumula-

tive waiting time distribution in both control and toxin conditions was biphasic with a fast component with time constant of ~3 ms (area = 0.6–0.7). Toxin-modified channels, however, had a second component that was twice as slow as that of control. This means that at −50 mV, modified channels open for the first time very late in the test pulse at a time when normal channels have inactivated, which suggests that TsIV-5 also alters the transition from closed to inactivated states.

The effects of α scorpion toxins such as *Leirus quinquestriatus V* on neuronal Na channels have been shown previously to be partly relieved by depolarization of the holding potential (e-fold decrease/19 mV over the range −100 to 0 mV; Gonoi et al., 1984) or repetitive stimulation at high frequency (e.g., test pulse to +100 mV at 2 Hz; Strichartz and Wang, 1986). Under our experimental conditions, voltage-

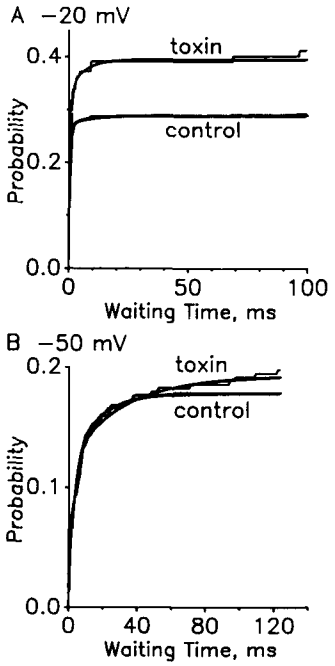

FIGURE 8. Frequency distribution of waiting times in the absence and presence of TsIV-5. Cumulative waiting times were corrected for four channels by the method of Patlak and Horn (1982). Same experiment as in Fig. 5. Smooth curves are biexponential functions with the following parameters. (*A*) Control time constants (and weighting factors), 0.59 ms (0.95) and 9.23 ms (0.05); toxin time constants, 0.65 ms (0.84) and 6.14 ms (0.16). (*B*) Control time constants, 3.01 ms (0.66) and 16.08 ms (0.34); toxin time constants, 2.90 ms (0.64) and 32.48 ms (0.36).

dependent dissociation did not cause time-dependent changes in the toxin effect. In the whole-cell experiments shifting the holding potential from −120 to −80 mV (Fig. 2) or repetitive pulsing to +70 mV at 0.2 Hz (not shown) caused no change in the toxin-induced prolongation of the inactivation phase. In the single-channel experiments pulses were delivered in trains usually consisting of 58 pulses at a pulse repetition rate of 0.6 Hz. Fig. 9 shows that frequency-dependent effects did not occur under this stimulus regime. In this experiment 81 test pulses to −20 mV were delivered at 0.6 Hz. The membrane patch had previously equilibrated in 2×10^{-6} M TsIV-5 before pulsing. Fig. 9 shows a sequential trace-by-trace analysis of the proportion of open time, P_o, for N channels (NP_o, ordinate). High NP_o traces, consisting of long-lasting bursts of activity, were distributed evenly throughout the recording period, indicating that no time-dependent change in toxin effect occurred.

The effects of TsIV-5 are not restricted to neuroblastoma Na channels. As shown

in Fig. 10, toxin application caused a similar pattern of channel bursting and prolonged open times in other Na channels representing the three major mammalian subgroups, namely brain (represented by cortical neurons from neonatal rat, Fig. 10 *A*), skeletal muscle (C2 myotubes derived from mouse myoblasts, Fig. 10 *B*), and heart (ventricular myocytes from neonatal rat). Although a quantitative comparison of the effects of TsIV-5 on channel subtypes was not attempted, it is clear from Fig. 10 that all three types are sensitive to this toxin even though they are known to differ in their sensitivities to tetrodotoxin and μ-conotoxin (Cruz et al., 1985).

DISCUSSION

The α scorpion toxins are believed to interact specifically with the inactivation mechanism of Na channels. The main conclusion of our study is that TsIV-5 exhibits the electrophysiological characteristics of an α toxin and that this class of toxins selectively inhibits inactivation gating at both the macroscopic and single-channel levels. Thus, the effects of TsIV-5 on Na current in neuroblastoma resemble those of Tityustoxin previously reported by Barhanin et al. (1982) to potentiate veratrid-

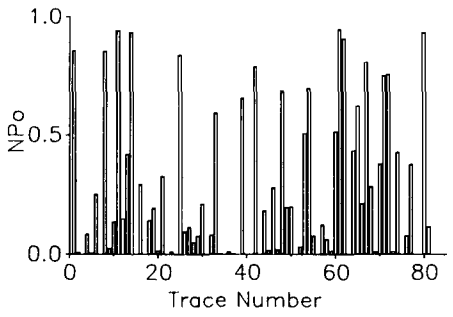

FIGURE 9. Diary analysis of proportion of open time in sequential traces after equilibration in 2×10^{-6} M TsIV-5 in a previously unstimulated outside-out patch. Proportion of open time per 140 ms trace, P_o, for N channels is plotted on the ordinate vs. trace number on the abscissa. Test pulse, -20 mV; holding potential, -90 mV. Temperature was 9.9°C.

ine-stimulated Na influx in rat brain synaptosomes. In that study Tityustoxin also was shown to bind to a different site from Ts-γ, the latter toxin belonging to the β class (Vijerberg et al., 1984; Yatani et al., 1988). Under whole-cell recording conditions, we find that TsIV-5 caused a prolongation of the decay phase, an increase in peak, and virtually no change in the time-to-peak of macroscopic currents evoked by test potentials more positive than -40 mV. Our results appear to be in good agreement with those of Gonoi and Hille (1987) who have recently described the effects of a variety of inactivation modifiers including the α toxin from *Leirus quinquestriatus* on macroscopic Na currents in neuroblastoma cells. They argue that because of the overlap between the time course of activation and inactivation, any agent that inhibits inactivation will cause an increase in peak current and a negative shift of the peak conductance-voltage curve along the voltage axis. The effects of TsIV-5 strongly corroborate their results and extend the analysis to the single-channel level.

Based primarily on analysis of single-channel currents, TsIV-5 appears to modify the transition from open to inactivated channel states. In contrast, we have shown previously that β toxins such as Ts-γ, modify gating transitions between closed and open states (Yatani et al., 1988). In the following section we develop a kinetic model

consistent with the notion that α toxins modify single channels by inhibiting transitions into the inactivated state.

For simplicity we will deal with the effects of toxin on P_o, open time, and bursting. Fig. 11 illustrates both the model and the resulting simulated Na currents. In the kinetic scheme we assume that normal channels reside initially in state C_1 and upon step depolarization to -20 mV proceed sequentially through two closed states (C_2 and C_3), a single open state (O_4), and finally into a single absorbing inactivated state (I_5). Pathways from closed to inactivated states are provided to account for null traces in which channels inactivate without opening. To simplify calculation, forward rates k_{12} and k_{23} were assumed to be equal; also, the backward rates k_{21} and k_{32} were set equal. Transitions into the inactivated state were assumed to be irreversible.

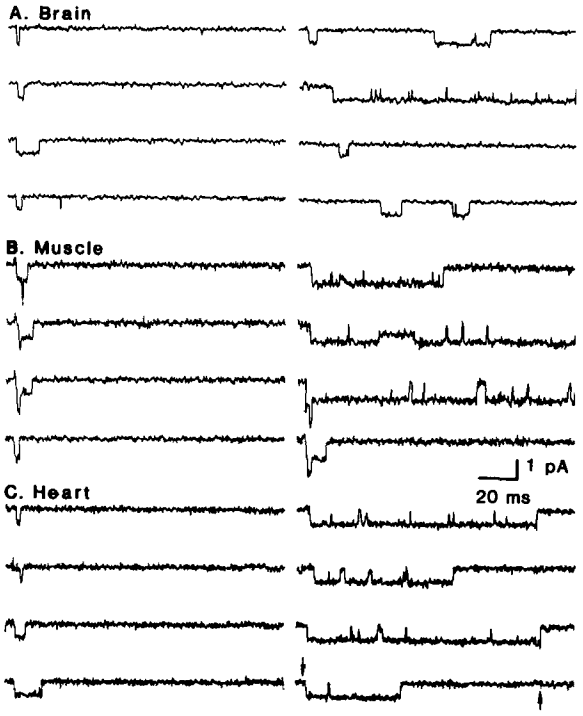

FIGURE 10. Effects of TsIV-5 on mammalian Na channels from brain, muscle, and heart. (*A*) Cortical neuron neonatal rat. (*B*) Myotube from mouse-derived skeletal muscle cell line C2. (*C*) Ventricular myocyte from neonatal rat. All data were obtained under recording conditions similar to those of Fig. 5, at a test potential of -20 mV from holding potentials of -90 (*A*) and -120 (*B* and *C*). Toxin concentrations 4×10^{-7}, 3×10^{-7}, and 4×10^{-6} M, respectively, in *A*, *B*, and *C*.

The toxin P_o curve was fit by the following procedure. In this model the mean open time of normal channels is determined by k_{45} and k_{43}. The toxin-induced prolongation of mean open time can be achieved by reducing k_{45}, then mean open time approaches $1/k_{43}$, which can be calculated from the toxin data. Rate k_{34} is obtained from 1/mean closed time within toxin-induced bursts. Rate k_{32} was calculated from the number of closed intervals in the burst (Fenwick et al., 1983). The remaining rate constants were fit to the toxin P_o curve by an iterative procedure. The control P_o curve was fit by constraining all rates to equal those of the toxin model except k_{45} and k_{35}, which were obtained by curve-fitting, with the result that, according to the model the toxin completely inhibited the transition from O_4 to I_5 and reduced k_{35} twofold. As shown in Fig 11 *A* the simulated P_o curves predict the observed toxin-

induced increase in peak currents as well as the markedly prolonged decay phase. The simulated single-channel records closely resemble actual records (note the difference in time scale between Figs. 5 and 11), showing both prolonged open time and bursting. The mean open times were 1.7 and 5.0 ms, and mean burst durations were 2.2 and 21.9 ms, respectively, in control and toxin-simulated data. The accuracy of the simulation suggests that at this potential the main effect of the toxin is to prevent inactivation from the open state; the path from closed to inactivated states remains available and accounts for the slow decay of P_o (Figs. 1, 7 *B*, and 11 *A*). At more negative potentials the toxin has little apparent effect on open time and bursting since, according to this model, k_{43} is the major determinant of channel open

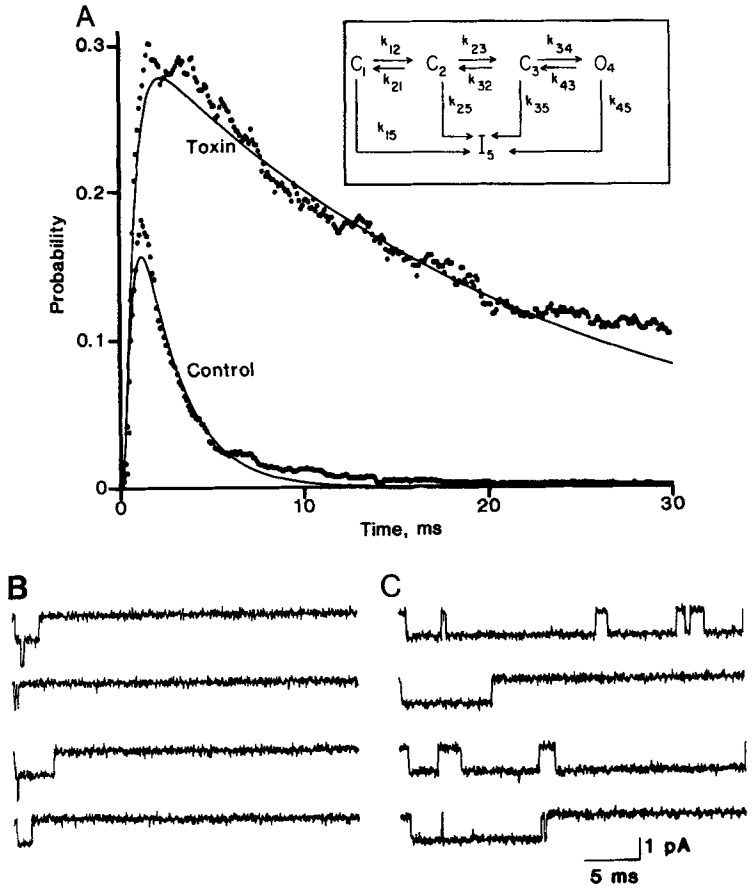

FIGURE 11. Model simulation of TsIV-5 effect on probability of single-channel opening (*A*) and single-channel bursting kinetics (*B* and *C*). Test potential −20 mV. In the kinetic model, rate constants that could be extracted directly from single-channel toxin data were constrained and the remaining rates were obtained by fitting the observed P_o to the model by an iterative curve-fitting procedure. In fitting the control P_o curve, all rate constants were constrained to equal those obtained in the toxin data, except k_{45} and k_{35} which were fit. The rate

time, and inactivation proceeding from closed channels is only moderately affected.

Gonoi and Hille (1987) have shown that a simpler model consisting of irreversible transitions from closed to open to inactivated states can account for the effects of a variety of inactivation modifiers on macroscopic Na currents in neuroblastoma. In this model, as in the Aldrich-Corey-Stevens model (1983), the transition from open to inactivated states is rapid and voltage independent compared with transitions among closed states and from closed to open states. Such a model accurately predicts that a toxin-induced decrease in the rate of transit from open to inactivated states will result in a slowing of macroscopic inactivation particularly at more positive test potentials, since long waiting times rather than long open times dominate the decay phase at test potentials near threshold. The model has the drawback, however, of incorrectly predicting that mean open times in toxin-modified channels will be uniformly longer at all test potentials. As shown in Fig. 7, at a test potential of −60 mV the mean open time of toxin-modified channels is the same as in control, which suggests that the transition from open to closed is reversible and not significantly altered by toxin binding. A similar conclusion was reached by Carbone and Lux (1986) from the effects of pronase on single Na currents in dorsal root ganglion neurons.

Our model, however, is incomplete in several respects since it does not account for the observed holding potential dependence of channel availability (Fig. 2) and the biphasic open-time histograms (Fig. 6 *B*). The first effect is similar to, albeit less drastic than, the channel "hibernation," which results from other treatments that remove fast inactivation (Patlak and Horn, 1982) and implies that the toxin-modi-

---

parameters obtained by the fitting procedure were used to generate the simulated single-channel data (*B* and *C*). Rate constants used in simulation (1/s):

Rate	Control	Toxin
k_{12}	4,157	4,157
k_{21}	147	147
k_{23}	4,157	4,157
k_{32}	147	147
k_{34}	1,470	1,470
k_{43}	220	220
k_{15}	1,803	1,803
k_{25}	2,505	2,505
k_{35}	1,045	404
k_{45}	392	0

Kinetic parameters calculated from simulated (and real) data:

Parameter	Control	Toxin
Mean open time (ms)	1.6 (1.1)	4.5 (4.5)
Mean intraburst closed time (ms)	0.4 (0.9)	0.4 (0.8)
Mean burst duration (ms)	2.2 (2.4)	21.6 (29.5)
Number of openings per burst	1.2 (1.3)	4.1 (4.0)

fied channel can enter long-lived inactivated states (e.g., "ultra-slow" inactivation; Fox, 1976) more readily than normal channels. The second effect implies that the toxin-modified channel has more than one open state, each having the same unitary conductance but differing in dwell time. In neuroblastoma, Nagy (1987) has presented compelling eivdence that two open states exist even in normal channels. Our open-time histograms for unmodified channels can be accurately fit to a monophasic decay, however, a second open state may be difficult to resolve in the presence of multiple channels. TsIV-5, by inhibiting inactivation, may increase the probability of observing a second open state. Quandt (1987) has made similar observations in neuroblastoma treated intracellularly with papain to remove inactivation, which suggests that multiple open states are unmasked by toxin rather than being the direct result of toxin modification of the channel.

In conclusion, our results provide a description of α scorpion toxin action that is consistent with a selective, toxin-induced modification of the inactivation gating mechanism. Together with information concerning the location of the α toxin–binding site within the primary and secondary structures of the Na channel protein, this result should provide an important constraint on models that explain Na channel structure-function relationships.

We thank Dr. A. M. J. VanDongen for making available the rate-fitting program used for kinetic modelling.

This work was supported by American Heart Association grant 876197 to G. E. Kirsch and by National Heart, Lung and Blood Institute grants HL-07696 to A. Skattebøl, and HL-25143 and HL-33662 to A. M. Brown.

Original version received 26 March 1988 and accepted version received 7 July 1988.

REFERENCES

Aldrich, R. W., D. P. Corey, and C. F. Stevens. 1983. A reinterpretation of mammalian sodium channel gating based on single channel recording. *Nature.* 306:436–441.

Barhanin, J., J. R. Giglio, P. Leopold, A. Schmid, S. V. Sampaio, and M. Lazdunski. 1982. *Tityus serrulatus* venom contains two classes of toxins. *Journal of Biological Chemistry.* 257:12553–12558.

Carbone, E., and H. D. Lux. 1986. Sodium channels in cultured chick dorsal root ganglion neurons. *European Biophysical Journal.* 13:259–271.

Colquhoun, D., and B. Sakmann. 1985. Fast events in single-channel currents activated by acetylcholine and its analogues at the frog muscle end-plate. *Journal of Physiology.* 369:501–557.

Couraud, F., E. Jover, J. M. Dubois, and H. Rochat. 1982. Two types of scorpion toxin receptor sites, one related to the activation, the other to the inactivation of the action potential sodium channel. *Toxicon.* 20:9–16.

Cruz, L. J., W. R. Gray, B. M. Oliveira, R. D. Zeikus, L. Ken, D. Yoshikami, and E. Moczydlowski. 1985. *Conus geographicus* toxins that discriminate between neuronal and muscle sodium channels. *Journal of Biological Chemistry.* 260:9280–9288.

Fenwick, E. M., A. Marty and E. Neher. 1983. Sodium and calcium channels in bovine chromaffin cells. *Journal of Physiology.* 331:599–635.

Fox, J. M. 1976. Ultra-slow inactivation of the ionic currents through the membrane of myelinated nerve. *Biochimica et Biophysica Acta.* 426:232–244.

Gomez, M. V., and C. R. Diniz. 1966. Separation of toxic components from the Brazilian scorpion *Tityus serrulatus* venom. *Memorias do Instituto Butantan.* 33:899–902.

Gonoi, T., and B. Hille. 1987. Gating of Na channels. Inactivation modifiers discriminate among models. *Journal of General Physiology.* 89:253–274.

Gonoi, T., B. Hille, and W. A. Catterall. 1984. Voltage clamp analysis of sodium channels in normal and scorpion toxin-resistant neuroblastoma cells. *Journal of Neuroscience.* 4:2836–2842.

Hamill, O. P., A. Marty, B. Sakmann, and F. J. Sigworth. 1981. Improved patch-clamp techniques for high-resolution current recording from cells and cell-free membrane patches. *Pflügers Archiv.* 391:85–100.

Hodgkin, A. L., and A. F. Huxley. 1952. A quantitative description of membrane current and its application to conduction and excitation in nerve. *Journal of Physiology.* 117:500–544.

Lux, H. D., and A. M. Brown. 1984. Patch and whole cell calcium currents recorded simultaneously in snail neurons. *Journal of General Physiology.* 83:727–750.

Nagy K. 1987. Evidence for multiple open states of sodium channels in neuroblastoma cells. *Journal of Membrane Biology.* 96:251–262.

Patlak, J., and R. Horn. 1982. Effect of *n*-bromoacetamide on single sodium channel currents in excised membrane patches. *Journal of General Physiology.* 79:333–351.

Possani, L. D., B. M. Martin, J. Mochca-Morales, and I. Svendsen. 1981. Purification and chemical characterization of the major toxins from the venom of the Brazilian scorpion *Tityus serrulatus* Lutz and Mello. *Carlsberg Research Communications.* 46:195–205.

Possani, L. D., B. M. Martin, I. Svendsen, G. S. Rode, and B. W. Erickson. 1985. Scorpion toxins from *Centruroids noxius* and *Tityus serrulatus. Biochemical Journal.* 229:739–750.

Quandt, F. N. 1987. Burst kinetics of sodium channels which lack fast inactivation in mouse neuroblastoma cells. *Journal of Physiology.* 392:563–585.

Renaud, J. F., M. Fosset, H. Schweitz, and M. Lazdunski. 1986. The interaction of polypeptide neurotoxins with tetrodotoxin-resistant Na^+ channels in mammalian cardiac cells. Correlation with inotropic and arrhythmic effects. *European Journal of Pharmacology.* 120:161–170.

Strichartz, G., T. Rando, and G. K. Wang. 1987. An integrated view of the molecular toxinology of sodium channel gating in excitable cells. *Annual Review of Neuroscience.* 10:237–269.

Strichartz, G., and G. K. Wang. 1986. Rapid voltage-dependent dissociation of scorpion alpha-toxins coupled to Na channel inactivation in amphibian myelinated nerves. *Journal of General Physiology.* 88:413–435.

Vandenberg, C. A. and R. Horn. 1984. Inactivation viewed through single sodium channels. *Journal of General Physiology.* 84:535–564.

Vijverberg, H. P. M., D. Pauron, and M. Lazdunski. 1984. The effects of *Tityus serrulatus* scorpion toxin on Na channels in neuroblastoma cells. *Pflügers Archiv.* 401:297–303.

Wheeler, K. P., D. D. Watt, and M. Lazdunski. 1983. Classification of Na channel receptors specific for various scorpion toxins. *Pflügers Archiv.* 397:164–165.

Yatani, A., G. E. Kirsch, L. D. Possani, and A. M. Brown. 1988. Effects of New World scorpion toxins on single-channel and whole cell cardiac sodium currents. *American Journal of Physiology.* 254:H443–H451.